Published in final edited form as:
*Biochim Biophys Acta*. 2010 May ; 1801(5): 547–558. doi:10.1016/j.bbalip.2010.01.006.

# Evidence for Proteolytic Processing and Stimulated Organelle Redistribution of iPLA$_2$β

**Haowei Song**, **Shunzhong Bao**, **Xiaoyong Lei**, **Chun Jin**, **Sheng Zhang**, **John Turk**, and **Sasanka Ramanadham***
Mass Spectrometry Resource, Division of Metabolism, Endocrinology, and Lipid Research, Department of Medicine, Washington University School of Medicine, St. Louis, MO, 63110, U.S.A

## Abstract

Over the past decade, important roles for the 84–88 kDa Group VIA $Ca^{2+}$-independent phospholipase $A_2$ (iPLA$_2$β) in various organs have been described. We demonstrated that iPLA$_2$β participates in insulin secretion, insulinoma cells and native pancreatic islets express full-length and truncated isoforms of iPLA$_2$β, and certain stimuli promote perinuclear localization of iPLA$_2$β. To gain a better understanding of its mobilization, iPLA$_2$β was expressed in INS-1 cells as a fusion protein with EGFP, enabling detection of subcellular localization of iPLA$_2$β by monitoring EGFP fluorescence. Cells stably-transfected with fusion protein expressed nearly 5-fold higher catalytic iPLA$_2$β activity than control cells transfected with EGFP cDNA alone, indicating that co-expression of EGFP does not interfere with manifestation of iPLA$_2$β activity. Dual fluorescence monitoring of EGFP and organelle Trackers combined with immunoblotting analyses revealed expression of truncated iPLA$_2$β isoforms in separate subcellular organelles. Exposure to secretagogues and induction of ER stress are known to activate iPLA$_2$β in β-cells and we find here that these stimuli promote differential localization of iPLA$_2$β in subcellular organelles. Further, mass spectrometric analyses identified iPLA$_2$β variants from which N-terminal residues were removed. Collectively, these findings provide evidence for endogenous proteolytic processing of iPLA$_2$β and redistribution of iPLA$_2$β variants in subcellular compartments. It might be proposed that *in vivo* processing of iPLA$_2$β facilitates its participation in multiple biological processes.

### Keywords

Golgi; ER; mitochondria; fusion protein; truncation; mass spectrometry

## 1. Introduction

Phospholipases $A_2$ ($PLA_2$)[1] are a diverse group of enzymes that catalyze hydrolysis of the *sn*-2 substituent from glycerophospholipid substrates to yield a free fatty acid and a 2-lysophospholipid [1–3]. Among the $PLA_2$s is a cytosolic $PLA_2$ that does not require $Ca^{2+}$ for catalysis and is designated Group VIA $PLA_2$ or iPLA$_2$β [4,5]. At present two variants of iPLA$_2$β are recognized and they are designated Group VIA-1 (84 kDa) and Group VIA-2 (88



*Corresponding Author's Address: Sasanka Ramanadham, Ph.D., Washington University School of Medicine, Department of Medicine, Box 8127, 660 S. Euclid Avenue, St. Louis, MO 63110, 314-362-8194; 314-362-7641 (Fax); sramanad@dom.wustl.edu.

kDa). The iPLA$_2$β enzyme is expressed in various organs, stimulated by ATP, and inactivated by a bromoenol lactone (BEL) suicide substrate inhibitor of iPLA$_2$β [6].

The iPLA$_2$β variants contain 7–8 NH$_2$-terminal ankyrin repeats, a caspase-3 cleavage site, an ATP-binding domain, a serine lipase consensus sequence (GXSXG), a bipartite nuclear localization sequence, a COOH-terminal calmodulin-binding domain(s) [6], and an ability to form a signaling complex with CamKIIβ [7]. Though regulation of iPLA$_2$β during stimulation is not well-understood, the iPLA$_2$β gene contains a sterol regulatory element (SRE) and binding of SRE binding proteins (SREBPs) to the SRE has been reported to promote iPLA$_2$β transcription [8]. The Group VIA-2 iPLA$_2$β, which is also expressed in human pancreatic islets, is the product of an mRNA species that arises from alternate splicing and contains a 54-amino acid sequence that interrupts the eighth ankyrin repeat [9].

The iPLA$_2$β enzyme is proposed to be involved in phospholipid remodeling [10], signal transduction [11–16], sperm motility and fertility [17], bone formation [18], and fatty acid oxidation in skeletal muscle [19]. Recently, a role for iPLA$_2$β in modulation of neurotransmission in the hippocampus [20], impairment in memory acquisition [21], nerve degeneration [22,23], infantile neuroaxonal dystrophy [24,25], schizophrenia [26,27], muscle degeneration [28], skeletal muscle contractility [29], HIV-induced cardiomyopathy [30], exfoliation glaucoma [31], and onset of acute pleurisy [32] has also been recognized. Further, over 30 studies during the past five years have linked iPLA$_2$β with apoptosis.

Studies in our laboratory reveal that pancreatic islet β-cells, but not non-βcells, express the Group VA-1 iPLA$_2$β that participates in insulin secretion [33–36], cell proliferation [4], and apoptosis [37–39]. In support, inhibition or knockdown of iPLA$_2$β suppresses [33,34,36,37, 40,41] and overexpression of iPLA$_2$β amplifies these effects [37,42,43]. However, these protocols do not affect β-cell membrane phospholipid remodeling [4,40,42,44], indicating a signaling role for iPLA$_2$β in the β-cell.

Curiously, β-cells express different isoforms of iPLA$_2$β protein that are not products of alternate splicing of the iPLA$_2$β transcript and that are catalytic activity. These include a 70 kDa protein that results from truncation of C-terminal amino acids [34] and a 63 kDa protein that is generated by caspase-3-catalyzed cleavage of N-terminal amino acids [45]. Immunocytochemistry analyses suggested that in the presence of certain stimuli, the Group VA-1 iPLA$_2$β localizes in the perinuclear region [45]. Subsequent expression of the Group VA-1 iPLA$_2$β in INS-1 cells as a fusion protein (fp) with EGFP revealed a predominant localization of iPLA$_2$β in the ER and Golgi [46].

In view of the presence of isoforms that result from truncation at either terminus of iPLA$_2$β, herein, we compared the localization of the Group VA-1 iPLA$_2$β expressed as a fusion protein. To facilitate identification of specific subcellular organelle(s) with which iPLA$_2$β might associate during such stimulation, we engineered INS-1 cells that express iPLA$_2$β as a fusion protein with EGFP fused to iPLA$_2$β either at its C-terminus ($^{N}$iPLA$_2$β-EGFP$^{C}$, designated fpN2) or at its N-terminus ($^{N}$EGFP-iPLA$_2$β$^{C}$, designated fpC2). Expression of iPLA$_2$β as a fusion protein permits tracking subcellular localization of iPLA$_2$β by monitoring EGFP green fluorescence.

[1]**ABBREVIATIONS**

Abbreviations used in this manuscript are: BEL, bromoenol lactone suicide substrate inhibitor of iPLA$_2$β; BSA, bovine serum albumin; C2 and N2, EGFP-C2 and EGFP-N2 vectors, respectively; ECL, enhanced chemiluminescence; EGFP, enhanced green fluorescence protein; ER, endoplasmic reticulum; fp, iPLA$_2$β/EGFP fusion protein; fpC2, $^{N}$EGFP-iPLA$_2$β$^{C}$ fusion protein; fpC2, $^{N}$iPLA$_2$β-EGFP$^{C}$ fusion protein; iPLA$_2$β, Group VIA $Ca^{2+}$-independent phospholipase A$_2$; kDa, kilodaltons; MS, mass spectrometry; OE, iPLA$_2$β overexpressing cells; O/N, overnight; PAGE, polyacrylamide gel electrophoresis; PLA$_2$, phospholipase A$_2$; PM, plasma membrane; Q-TOF, Quadrupole-time of flight; SDS, sodium dodecyl sulfate; and RT, room temperature

## 2. Materials and methods

### 2.1. Materials

INS-1 β-cells were generously provided by Dr. C. Newgard (Duke University Medical Center, Durham, NC). Other materials were obtained from the following sources: rainbow molecular mass standards and enhanced chemiluminescence (ECL) reagent (Amersham, Arlington Heights, IL); sodium dodecyl sulfate-polyacrylamide gel electrophoresis (SDS-PAGE) supplies (BioRad, Hercules, CA); pEGFP-N2 and pEGFP-C2 vectors (Clontech, Palo Alto, CA); GenePORTER™ transfection reagent (Gene Therapy Systems Inc., San Diego, CA); pentex fraction V fatty acid-free bovine serum albumin (Miles Laboratories, Eckert, IN); Golgi Tracker BODIPY® TR ceramide, ER-Tracker™ Blue-White DPX (E-12353), Mito Tracker Deep Red 633, plasma membrane Tracker DiI, and Slow Fade® light antifade kit (Molecular Probes, Eugene, OR); (16:0/[$^{14}$C]-18:2)-GPC (PLPC, 55 mCi/mmol), Coomassie reagent (Pierce, Rockford, IL); modified trypsin (Promega Corp., Madison, WI); peroxidase-conjugated goat anti-rabbit IgG antibody (Roche Diagnostic Corporation, Indianapolis, IN); primary antibodies against iPLA$_2$β and GFP, GFP (B-2) mouse monoclonal IgG$_{2α}$,, and goat anti-mouse IgG-HRP (Santa Cruz Biotechnology, Inc., Santa Cruz, CA); albumin, β-mercaptoethanol, protease inhibitor cocktail (PIC), and common reagents and salts (Sigma Chemical Co., St. Louis, MO); and antibiotic solutions and cell culture media (Tissue Culture Support Center, Wash. Univ., St. Louis, MO).

### 2.2. Preparation and expression of iPLA$_2$β as a fusion protein with EGFP in INS-1 cells

Vectors pEGFP-N2 and pEGFP-C2 encode a red-shifted variant of wild-type GFP [47] that have been optimized for brighter fluorescence and higher expression in mammalian cells. INS-1 cells overexpressing a fused protein were generated as described [46]. Briefly, cDNA encoding the full-length Group VIA-1 iPLA$_2$β (NP_058611) was amplified by PCR using the following primer set: sense, 5'-AGCTTCGAAT TCATGCAGTTCTTTGGACGC-3', and antisense, 5'-TTCGATATCGGGAGATAGCAGCAGCTGG-3'. The amplified full-length iPLA$_2$β from the pMSCV-neo- iPLA$_2$β constructs were then subcloned into the pEGFP-N2 and pEGFP-C2 (Clontech, Palo Alto, CA). Control vectors (pEGFP-N2 and pEGFP-C2), and constructs encoding fusion protein (fp) were transfected into INS-1 cells with a Gene PORTER transfection system, according to the manufacture's instructions (Gene Therapy Systems, San Diego, CA). Stably-transfected clones were selected using G418 (0.4 mg/ml) and fluorescence-activated cell sorting was utilized to optimize selection of stably-transfected cells with the highest iPLA$_2$β expression. The cells were expanded in RPMI 1640 medium containing 11 mM glucose, 10% fetal calf serum, 10 mM HEPES buffer, 2 mM glutamine, 1 mM sodium pyruvate, 50 mM β-mercaptoethanol, and 0.1% (w/v) each of penicillin, fungizone, and streptomycin [4,45]. Cells expressing EGFP-N2 and EGFP-C2 alone are designated N2 and C2, respectively, and were used as controls. Cells expressing iPLA$_2$β as a fusion protein with EGFP were designated fpN2 (EGFP fused at the C-terminus) and fpC2 (EGFP fused at the N-terminus).

### 2.3. Preparation of INS-1 cell subcellular fractions for iPLA$_2$β enzyme activity assays

INS-1 cell cytosol and membrane fractions were prepared and specific $Ca^{2+}$-independent PLA$_2$β activity in 25 μg protein aliquots was assayed in the presence of (16:0/[$^{14}$C]-18:2)-GPC substrate and quantitated, as described [48]. To verify that the measured activity reflected that of iPLA$_2$β, the abilities of ATP (10 mM) to stimulate and of BEL (10 μM) to inhibit activity were examined. To test the effects of BEL on activity, the sample protein was first pre-incubated (2 min, RT) with BEL before addition of substrate.

### 2.4. Secretagogue-stimulated translocation of iPLA$_2$β

To examine if secretagogues induce translocation of iPLA$_2$β, control and fusion protein expressing INS-1 cells were stimulated with glucose (G, 0 or 2 mM) in the absence and presence of forskolin (FSK, 2.5 μM). At 2 h, localization of iPLA$_2$β, as reflected by EGFP, was visualized by fluorescence microscopy using a FITC filter.

### 2.5. Secretagogue-stimulated subcellular localization of iPLA$_2$β

To identify organelles with which iPLA$_2$β associates, fluorescences of EGFP and of specific organelle Trackers were monitored in live control and fusion protein-expressing cells after secretagogue stimulation using an inverted microscope (Nikon Eclipse TE300). The fluorescence images were captured using Soft Imaging System software (Lakewood, CO) and merged using Adobe Photoshop Software. Protocols with the different Trackers were as follows:

**Golgi—**Cells were incubated (4 °C, 30 min) with 5 μM ceramide-BSA (BODIPY® TR ceramide), washed, and incubated (37 °C, 1 h) in cu lture medium containing zero glucose and 0.1% BSA. The cells were then incubated (37 °C) in med ium supplemented with 2 mM glucose and 2.5 μM forskolin for up to 2 h. At various times during stimulation, EGFP and the Golgi Tracker (rhodamine) fluorescences were monitored.

**ER, mitochondria, and plasma membrane—**Cells were initially washed and incubated (37 °C, 1 h) in medium containing zero glucose and 0.1% BSA. The medium was then replaced with one supplemented with 2 mM glucose and 2.5 μM forskolin for up to 2 h. The ER (Blue-White DPX 600 nM), mitochondrial (Deep Red 633), or plasma membrane (Dil D-282) Tracker was added to the medium during the final 30 min of incubation. At 2 h, the medium was replaced with one not containing a Tracker and iPLA$_2$β -associated EGFP fluorescence was monitored along with fluorescence associated with the ER (DAPI filter), mitochondria (rhodamine filter), or plasma membrane (rhodamine filter) Tracker.

### 2.6. ER stress-induced subcellular distribution of iPLA$_2$β

Our earlier work indicated that inducing ER stress promotes activation of iPLA$_2$β in the ER and mitochondria, leading to the release of cytochrome *c* and promoting apoptosis [38,39, 49]. To determine if this process involves translocation of iPLA$_2$β into the ER and/or mitochondria, a retroviral construct encoding a recombinant fusion protein consisting of EGFP attached to the N-terminus of the iPLA$_2$β sequence (fpC2) was prepared and used to generate stably-transfected INS-1 cells as previously described [46]. Fusion proteins containing fluorescent tags attached to marker proteins for subcellular organelles were expressed for co-localization studies. The plasmid expressed to track ER encoded a fusion protein of the ER-targeting sequence of calreticulin attached to the N-terminus of MonoRed (Clontech, Mountain View, CA). The plasmid expressed to track mitochondria encoded a fusion protein of the mitochondrial-targeting sequence of human cytochrome c oxidase subunit VIII attached to *Discosoma sp.* red fluorescent protein (DsRed2). To compare the subcellular distribution of the tagged iPLA$_2$β to that of the organelle markers, fpC2-expressing cells were transfected with either the pMonoRed-ER or the pDsRed2-Mito plasmid. To examine subcellular redistribution of the tagged iPLA$_2$β upon induction of ER stress, cells were incubated with thapsigargin (1 μM, 37 °C) for various intervals. Cells were then fixed and visualized and analysed, as described above.

**Preparation of mitochondria and ER fractions—**To identify the iPLA$_2$β isoforms that accumulate in the mitochondria and ER. Cells expressing iPLA$_2$β with EGFP fused at the C-terminus (fpN2) were treated with vehicle (DMSO) alone or thapsigargin and harvested at 5

and 8 h. Mitochondria and ER fractions were then prepared and aliquots (30 μg protein) were processed for immunoblotting analyses, as described [38,39].

### 2.7. Immunoblotting analyses

INS-1 cellular protein aliquots (30 μg) were analyzed by SDS-PAGE (7.5%), and processed for immunoblotting analyses as described [38,39]. Immunoreactive protein bands were visualized by enhanced chemiluminescence (ECL). The primary antibodies were directed against GFP ($IgG_{2\alpha}$, 0.0002 μg/μl) or $iPLA_2\beta$ (0.0015 μg/μl). The secondary antibodies were goat anti-mouse IgG-HRP (1:2,000) for GFP and peroxidase-conjugated goat anti-rabbit IgG (1:40,000) for $iPLA_2\beta$.

### 2.8. Mass spectrometric analyses of $iPLA_2\beta$

To determine whether $iPLA_2\beta$ undergoes endogenous proteolytic processing, $iPLA_2\beta$ overexpressed in INS-1 cells was purified, concentrated, digested with trypsin, and analysed by MS, as described [34]. Briefly, $iPLA_2^{®}$ was purified using ATP affinity chromatography. Fractions containing $iPLA_2^{®}$ activity were pooled and concentrated. The concentrate was then resolved by SDS-PAGE. Protein bands were visualized by Coomassie stain and the band in the region of 85 kDa, corresponding to the molecular mass of $iPLA_2^{®}$ was excised, reduced with 20 mM DTT and incubated with 50 mM iodoacetamide to alkylate the cysteine residue. Mass spectrometry grade trypsin (50:1) was then added and the gel pieces were incubated for 6 h at 37 °C. The digest was then centrifuged and the gel extract was injected into CapLC-Qtof (Waters) for data-dependent MS/MS analyses. Masslynx software was used to extract the peak list file from the MS/MS spectra. The peak list was then compared against a list of expected and unexpected peptides generated by a Signature Discovery Algorithm program recently developed in our laboratory [50]. These analyses facilitate identification of “signature” peptides derived from protein isoforms that reflect proteolytic processing events.

## 3. Results

### 3.1. Expression of $iPLA_2\beta$ enzymatic activity in INS-1 cells transfected with EGFP- $iPLA_2\beta$ cDNA

To confirm that the fpN2- and fpC2- transfected cells express a catalytically-active $iPLA_2\beta$ enzyme, cytosol and membrane fractions prepared from these cells were assayed for $Ca^{2+}$-independent $PLA_2$ activity. As shown in Fig. 1, both fpN2- and fpC2-expressing cells express a $Ca^{2+}$-independent $PLA_2$ activity that is four-to-five fold higher than that expressed in N2 and C2 cells. Such activity is stimulated by ATP and inhibited by BEL, which are recognized properties of $iPLA_2\beta$ [34,36,44,45,51]. These findings indicate preservation of $iPLA_2\beta$ activity when it is expressed as a fusion protein with EGFP.

### 3.2. Secretagogue-stimulated localization of $iPLA_2\beta$

We previously observed using immunofluorescence analyses that exposure to secretagogues promotes translocation of $iPLA_2\beta$ to the perinuclear region of INS-1 cells [45]. Because potential antibody nonspecificity can lead to misinterpretation of immunofluorescence experiments, $iPLA_2\beta$ was expressed in INS-1 cells as a fusion protein (fp) with EGFP, and its subcellular redistribution after secretagogue stimulation was monitored by fluorescence microscopy. Our findings with the N2 construct, reported earlier [45], revealed that under non-stimulating conditions the green fluorescence in cells expressing N2 and fpN2 is dispersed throughout the cell. Following addition of glucose (2 mM) plus forskolin (2.5 μM), which was sufficient to increase insulin secretion 2-fold (data not shown), the fluorescence remains dispersed in the N2 expressing cells but in the fpN2 expressing cells, punctuated $iPLA_2\beta$-associated green fluorescence is seen as a halo in the perinuclear region. Analogous analyses

in the present study in cells expressing C2 and fpC2 (Fig. 2) reveal a similar dispersion of fluorescence under non-stimulatory conditions. Upon stimulation, in contrast to what was observed in the fpN2 cells, a punctate fluorescence that is dispersed in the cytosol is seen.

### 3.3. Secretagogue-stimulated subcellular redistribution of iPLA$_2$β

To determine whether secretagogue stimulation of INS-1 cells promotes association of iPLA$_2$β with specific subcellular compartments, dual fluorescence analyses using organelle Trackers were next performed. Targeted organelles were the Golgi, ER, mitochondria, and plasma membrane. The cells were treated with glucose and forskolin, and, at appropriate times, an individual organelle Tracker was added to the medium. The EGFP (FITC) and organelle Tracker fluorescences were then recorded in a field of cells. In Fig. 3, the separate iPLA$_2$β-associated EGFP and organelle Tracker fluorescences are shown in the left and middle panels, respectively, and the overlays of the two fluorescences are shown in the right panels. Captured images were processed to reduce background fluorescence.

In our earlier study, we found that the green fluorescence associated with iPLA$_2$β in fpN2-expressing localized in the Golgi and ER, minimally associated with the plasma membrane, and not at all present in the mitochondria [45]. In contrast, as illustrated in Figure 3, the iPLA$_2$β fluorescences in fpC2 expressing cells did not appear to overlap with any of the organelle trackers. In view of the findings with fpN2, the present observations with fpC2 raise the possibility that the presence of EGFP at one of the terminus of iPLA$_2$β or possible proteolytic cleavage of the iPLA$_2$β may contribute to distinct cellular redistribution of iPLA$_2$β in secretagogue-stimulated β-cells.

### 3.4. Immunoblotting analyses provides evidence for endogenous processing of iPLA$_2$β

To examine the possibility that iPLA$_2$β undergoes endogenous proteolytic processing, cytosol prepared from fp-expressing cells was processed for immunoblotting analyses using antibodies against EGFP and iPLA$_2$β. As illustrated in Fig. 4A, cells transfected with the EGFP-alone vector (N2 and C2) express only the EGFP-immunoreactive bands ca. 26 kDa (N2) and 29 kDa (C2), where the difference in mass is due to differences in the length of the insert encoded by the two vectors (left panel). The expected size of the fp, comprising EGFP and full-length iPLA$_2$β (84 kDa) therefore is 110–113 kDa. However, immunoblotting analyses of cytosol from INS-1 cells expressing $^{N}$iPLA$_2$β-EGFP$^{C}$ (fpN2) and $^{N}$EGFP-iPLA$_2$β$^{C}$ (fpC2) revealed additional EGFP-immunoreactive bands that migrated with apparent molecular masses of ca. 90 kDa (fpN2) and 100 kDa (fpC2) (Fig. 4A, right panel). These bands appear to represent iPLA$_2$β variants, as they are also recognized by polyclonal antibodies against iPLA$_2$β (Fig. 4B). As seen in panel 4B, an additional iPLA$_2$β-immunoreactive band is evident at 70 kDa.

A potential rationale for the observed immunoreactive bands is presented in Fig. 4C. The 90 kDa EGP-immunoreactive band evident only in fpN2-expressing cells most likely represents a variant of iPLA$_2$β from which amino acid residues have been removed from the N-terminal region. As the EGFP is fused to the C-terminus of fpN2, this truncated isoform retains EGFP, is recognized by the EGFP antibody, and would exhibit fluorescence. In contrast, similar cleavage of fpC2 would result in the elimination of the EGFP that is fused to the iPLA$_2$β N-terminus. The product of this cleavage that retained the majority of the iPLA$_2$β sequence would thus fail to be recognized by EGFP antibody and to exhibit fluorescence, although it would react with iPLA$_2$β antibody. The 100 kDa EGFP-immunoreactive band that is evident only in the fpC2-expressing cells probably represents a variant of iPLA$_2$β from which 10–12 kDa of amino acid sequence has been removed from the C-terminal. As the EGFP in fpC2 is fused to the N-terminus of iPLA$_2$β, this truncated isoform is recognized by the EGFP antibody. In contrast, similar cleavage of fpN2 would result in the elimination of EGFP fused to the C-terminus of iPLA$_2$β, and this variant would not be recognized by the EGFP antibody.

Because the control cells (N2 and C2) are transfected with only the EGFP vectors and hence do not express a fusion protein, the iPLA$_2$β-immunoreactive bands seen in these cells (Fig. 4C) most likely represent endogenous full-length iPLA$_2$β produced from the transcripts of the native gene and a 70 kDa iPLA$_2$β variant produced by removal of about 14 kDa of C-terminal sequence [52].

Consistent with the fluorescence analyses, the plasma membrane fraction contains an immunoreactive band (ca. 110–113 kDa) that is recognized by both EGFP and iPLA$_2$β antibodies. This suggests that only the full-length iPLA$_2$β protein associates with plasma membranes (Fig. 5).

### 3.5. ER stress-induced redistribution of iPLA$_2$β between the ER and mitochondria

The findings that ER- and mitochondrial-associated iPLA$_2$β activities are increased following induction of ER stress with thapsigargin in INS-1 cells suggest that an interaction between iPLA$_2$β and the ER and mitochondria occurs during the evolution of apoptosis. To examine this further, INS-1 cells that express fpC2 and ER (calreticulin) or mitochondria (cytochrome *c* oxidase subunit VII) markers tagged to fluorophores were generated and visualized by fluorescence microscopy following vehicle or thapsigargin treatment. Individual fluorescence associated with iPLA$_2$β-tagged with EGFP (fpC2, left panels) and organelle markers (middle panels), and the merged fluorescences (right panels) are presented in Fig. 6 (ER) and Fig. 7 (mitochondria).

The choice of using the N-terminally tagged enzyme was based on the following: (1) We previously demonstrated that thapsigargin induces accumulation of full-length iPLA$_2$β in the ER [38] and then in the mitochondria [39], therefore we focused on potential translocation of this iPLA$_2$β isoform. (2) As illustrated in Fig. 4 above and reported earlier [34], iPLA$_2$β undergoes proteolytic processing at the C-terminal region *in vivo* to generate a 70 kDa isoform that is catalytically active. Tagging the C-terminal of iPLA$_2$β could potentially result in the loss of the EGFP label and hence, preclude the ability to visualize any potential translocation of the full-length protein.

As seen in Fig. 6, the merged image in the vehicle-treated group (top) exhibits a homogeneous yellow-orange color consistent with co-localization of fluorescences associated with iPLA$_2$β and ER marker calreticulin, suggesting that iPLA$_2$β is associated with ER under basal conditions. Following induction of ER stress, there is a time-dependent segregation of green fluorescence, suggesting that iPLA$_2$β undergoes subcellular redistribution away from the ER. In contrast, though control iPLA$_2$β fluorescence is prominent in Fig. 7, the merge image reveals that iPLA$_2$β fluorescence is not strongly associated with the mitochondrial tracker suggesting that interaction between iPLA$_2$β and mitochondria under basal conditions is minimal. However, following induction of ER stress the merged images reveal a time-dependent appearance of yellow-orange structures consistent with co-localization of fluorescences associated with iPLA$_2$β and mitochondrial marker cytochrome *c* oxidase subunit VII, suggesting that iPLA$_2$β undergoes progressive association with mitochondria.

### 3.6. ER stress-induced accumulation of iPLA$_2$β in the ER and mitochondria

We next sought to identify the iPLA$_2$β isoforms that accumulate in the mitochondria and ER. Because our earlier studies suggested that iPLA$_2$β in INS-1 cells undergoes proteolytic cleavage at the N-terminus during ER stress [37], we performed these studies using cells expressing iPLA$_2$β with EGFP fused at the C-terminus (fpN2). This allows detection of subcellular localization of iPLA$_2$β isoforms that might be cleaved at the N-terminus because they would remain fused to EGFP. The cells were treated with vehicle (DMSO) alone or thapsigargin and harvested at 5 and 8 h for immunoblotting analyses. Probing for either

iPLA$_2$β (data not shown) or EGFP (Fig. 8A) reveals a similar immunoreactive pattern where only one band migrating with an apparent molecular mass of ca. 110 kDa is evident. Because this mass is reflective of a full-length iPLA$_2$β fused to EGFP, these findings suggest that it is the full-length iPLA$_2$β that localizes in the mitochondria and ER during ER stress. And, consistent with the findings with the organelle Trackers, ER stress caused a progressive decrease in ER iPLA$_2$β and a concomitant increase in mitochondria-associated iPLA$_2$β (Fig. 8B).

### 3.7. Mass spectrometry analyses of iPLA$_2$β

To obtain further evidence of endogenous proteolytic processing, iPLA$_2$® was purified from INS-1 cells and analysed by mass spectrometry. Using LC-MS/MS analyses, we detected not only peptides expected after digestion of iPLA$_2$® with trypsin, but also a peptide arising from non-trypsin proteolytic processing. The doubly-charged ion at *m/z* 955.01 identified at retention time of 49 min (Fig. 9A) matches the theoretical molecular mass (1908.94 Da) of iPLA$_2$® tryptic peptide $^{7}$L-R$^{23}$, and MS/MS analysis (Fig. 9B) confirmed its amino acid sequence to be $^{7}$LVNTLSSVTNLFSNPFR$^{23}$.

As illustrated in Fig. 10A, at retention time 44 min, an abundant doubly-charged ion at *m/z* 791.90 was detected. However, this ion is not expected to arise from trypsin digestion of iPLA$_2$®. Processing its MS/MS spectrum (Fig. 10B) using a Signature Discovery Algorithm program [50] revealed that it represents TLSSVTNLFSNPFR (1581.82 Da), which is part of the tryptic peptide $^{7}$LVNTLSSV$^{10}$TNLFSNPFR$^{23}$. The detection of $^{10}$T-R$^{23}$ therefore reflects a “signature peptide” that derives from an iPLA$_2$β variant produced by *in vivo* proteolytic processing.

## 4. Discussion

The Group VIA phospholipase A$_2$ (iPLA$_2$β) is proposed to play a role in several biological processes [8]. In the β-cell, we reported participation of iPLA$_2$β in insulin secretion and apoptosis. Consistent with its involvement in these processes, inhibition or knock-out of iPLA$_2$β activity suppresses [33,35–41,52,53] and overexpression of iPLA$_2$β amplifies [37–39,42,43,45] secretagogue-stimulated insulin secretion and apoptosis.

In subsequent studies, insulin secretagogues were found to cause subcellular redistribution of iPLA$_2$β from the cytoplasm to the perinuclear region. These observations were derived from immunofluorescence experiments that in principle could be confounded by non-specificity of iPLA$_2$β antibodies and/or by cellular fixation artifacts [45]. To circumvent those issues iPLA$_2$β was express as a fusion protein (fp) with EGFP fused to either the N-terminus (EGFP-iPLA$_2$β, designated fpC2) or the C-terminus (iPLA$_2$β-EGFP, designated fpN2) of iPLA$_2$β, and subcellular localization within the β-cells was re-examined. INS-1 cells stably-transfected with the iPLA$_2$β/EGFP constructs expressed several-fold higher $Ca^{2+}$-independent PLA$_2$ enzymatic activity than cells stably-transfected with the EGFP vector alone. Such activity is inhibited by BEL and stimulated by ATP, and both properties are characteristic of iPLA$_2$β. This suggests that the fusion of EGFP to iPLA$_2$β does not interfere with manifestation of iPLA$_2$β catalytic activity.

The fusion of EGFP to iPLA$_2$β allowed us to track iPLA$_2$β movements within the cell by monitoring the green fluorescence of EGFP. The present findings reveal that stimulation of INS-1 cells that express iPLA$_2$β/EGFP with secretagogues causes the appearance of punctate areas of fluorescence that reflect a subcellular redistribution of iPLA$_2$β. Curiously, the punctate distribution of fluorescence differs between cells that express EGFP fused to the N-terminus compared to the C-terminus of iPLA$_2$β. In the fpN2-expressing cells, the punctate fluorescence accumulates in the perinuclear region, resembling the pattern observed with

immunofluorescence analyses [45]. In contrast, in the fpC2-expressing cells, the punctate area of fluorescence appears throughout the cytoplasm. Association of iPLA$_2$β with subcellular compartments was next examined in combination with fluorescent Trackers targeted at specific organelles and in contrast to the findings of fpN2 localization in the ER and Golgi, fpC2 did not appear to associate with the ER, Golgi, mitochondria, or plasma membrane.

The differential subcellular iPLA$_2$β localization in the fpN2- and fpC2-expressing cells is probably a reflection of endogenous processing of iPLA$_2$β and the presence or absence of amino acid sequences that might target iPLA$_2$β to specific subcellular organelles. The expected sizes of the fp are 110–113 kDa, of which EGFP accounts for 26–29 kDa and such bands are observed. Two additional EGFP-immunoreactive bands that migrate with apparent molecular masses of ca. 90 kDa and 100 kDa are also visualized. The 90 kDa band is evident only in fpC2-expressing cells, and the 100 kDa band only in fpN2-expressing cells. We reported that β-cells express at least two catalytically-active truncated isoforms of iPLA$_2$β; a 63 kDa isoform that is a product of caspase-3-mediated cleavage [37] and a 70 kDa isoform that arises from proteolytic removal of C-terminus sequence [34]. Interestingly, the 70 kDa iPLA$_2$β variant is the predominant isoform in parental INS-1 cells and native pancreatic islets.

Our observations here and elsewhere [34,37] are consistent with the possibility that the 90 kDa band represents the iPLA$_2$β variant that is produced by caspase-3 cleavage. As the EGFP is fused to the C-terminus of fpN2, the 90 kDa iPLA$_2$β caspase-3-cleavage product is still recognized by the EGFP antibody. Similar cleavage of the fpC2 would result in the loss of EGFP fused to the N-terminus of iPLA$_2$β, and this would prevent recognition by the EGFP antibody. Analogously, the 100 kDa iPLA$_2$β-EGFP band probably represents the fusion product of EGFP and that region of iPLA$_2$β contained in the native 70 kDa iPLA$_2$β isoform. Cleavage of C-terminal residues from fpN2 would result in the loss of EGFP fused to the C-terminus of iPLA$_2$β, and this would prevent recognition by the EGFP antibody. Collectively, these findings suggest that iPLA$_2$β undergoes post-translational proteolytic processing and that an isoform from which N-terminal sequence has been removed accumulates in the ER and Golgi following cell stimulation. The iPLA$_2$β isoform that forms a punctate distribution in the cytosol upon cell stimulation retains the N-terminus. The iPLA$_2$β isoform that accumulates in the ER and Golgi upon cell stimulation retains the C-terminus.

Stimulus-induced translocation of the Group V sPLA$_2$ and Group IV cPLA$_2$ to the perinuclear region has also been demonstrated [54,55], and cPLA$_2$ has been reported to translocate to the Golgi and/or ER depending on the stimulus [56]. In this regard, we recently found evidence of time-dependent accumulation of iPLA$_2$β protein in the ER, mitochondria, and nucleus of INS-1 cells following long-term (4–24 h) exposure to the SERCA inhibitor thapsigargin [37–39]. Consistent with these observations, organelle tracking analyses (Fig. 6 and Fig. 7) performed in the present study reveal that induction of ER stress in INS-1 cells promotes redistribution of iPLA$_2$β from the ER and its subsequent accumulation in the mitochondria. This is supported by immunoblotting analyses (Fig. 8) of isolated ER and mitochondrial fractions

However, it should be noted that the basal levels of iPLA$_2$β in the two fractions appear to be different depending on the analyses used. Results with the organelle Trackers suggest that basal ER accumulation of iPLA$_2$β is greater than in the mitochondria but the immunonoblotting findings, similar to our earlier observations [38,39], suggest the opposite. To reconcile this discrepancy, it is necessary to consider the fusion protein used in the two analyses. Organelle Trackers were used in cells expressing iPLA$_2$β fused to EGFP at the N-terminus and, as described above, proteolytic cleavage at the C-terminal end of this fusion protein would generate a truncated iPLA$_2$β protein. It might be speculated that this leads to deletion of a mitochondrial targeting sequence precluding accumulation of the truncated iPLA$_2$β in the mitochondria. It could be further speculated that induction of ER stress activates enzymes and/

or generates factors that inhibit proteolytic cleavage of iPLA$_2$β allowing the full-length iPLA$_2$β to translocate to the mitochondria. Because the immunoblotting analyses were performed using cells expressing iPLA$_2$β fused to EGFP at the C-terminus, it is plausible that this fusion protein is protected from proteolytic cleavage at the C-terminal and therefore is able to retain the mitochondrial targeting sequence. This would allow its localization in the mitochondria under basal conditions and its accumulation following induction of ER stress.

Interestingly, there appear to be differences in iPLA$_2$β localization following secretagogue stimulation and induction of ER stress. For instance, translocation events following exposure to secretagogue occur within 30 min and last up to 2 h. In contrast the onset of iPLA$_2$β mobilization after exposure to thapsigargin is later and lasts up to 20–24 h. Further, while the localization after secretagogue treatment concurrently appears predominantly in the ER and the Golgi, it proceeds from the ER to the mitochondria following ER stress induction. Additionally, we previously reported that ER stress induces nuclear association of iPLA$_2$β [45] and recently observed that ER stress induces iPLA$_2$β expression *(Lei et al., in press)*. To date, we have no evidence of nuclear accumulation or induction of iPLA$_2$β expression in INS-1 cells following secretagogue exposure. These findings suggest that the type and duration of stimulus can influence subcellular distribution of iPLA$_2$β.

The likelihood that iPLA$_2$β is processed endogenously was first evident from studies demonstrating that the 70 kDa protein was an iPLA$_2$β isoform that was truncated at the C-terminus and was not a product resulting from alternate splicing of the iPLA$_2$βtranscript [34]. Subsequently, we obtained evidence for other iPLA$_2$β variants that were truncated at various amino acid residues at the N-terminus [50,57]. In the present study, further evidence of iPLA$_2$β variants generated by endogenous proteolytic processing of iPLA$_2$β was obtained using a Signature Discovery Algorithm program developed in our laboratory to analyse peptide fragments identified by mass spectrometry protocols [50]. Analyses of tryptic digest of purified iPLA$_2$β by this method identified several peptide fragments arising from tryptic digestion of iPLA$_2$β. In addition to the expected fragments, however, a doubly-charged ion with *m/z* 791.90 is evident and this was identified by tandem mass spectrometry as having the amino acid sequence of $^{10}$T-R$^{23}$. Because this is an unexpected fragment, $^{10}$T-R$^{23}$ reflects a “signature peptide” that derives from an iPLA$_2$β variant produced by *in vivo* proteolytic processing.

The size of these proteolytic processed proteins are most likely 1–2 kDa smaller than the full length protein and this is deduced based on the following observations: (1) The identified N-terminal fragments arose from digestion of an iPLA$_2$β-immunoreactive band which migrated with an apparent molecular mass of ca. 80–84 kDa. (2) The protein was His-tagged at the C-terminus and was purified using a cobalt-affinity column and visualization of an iPLA$_2$β-immunoreactive band would only be possible if the His-tag was still present on the protein, allowing it to be eluted from the column. Thus, the fragments analysed by MS arose from a protein that spanned the N-terminal amino acids (minus the 1–2 kDa truncated residues) to the end of the C-terminal residues.

Though direct evidence is not yet available, the current observations raise the possibility that proteolytic processing of iPLA$_2$β may be a factor in its redistribution. Consistent with this possibility are the findings that iPLA$_2$β accumulates in different subcellular organelles under different conditions and differential localization is evident fpN2 and fpC2 following secretagogue stimulation. This raises the likelihood that the two termini contain potential targeting sequences that may be lost from the cleaved proteins. Future studies that will include expression of processed iPLA$_2$β isoforms to more directly track their mobilization following different stimuli should facilitate clarification of the affect of proteolytic processing on iPLA$_2$β translocation.

In summary, we find that iPLA$_2$β undergoes endogenous proteolytic processing and exhibits variable subcellular localization. Studies are currently underway to express the different iPLA$_2$β isoforms in INS-1 cells to determine the identities of the variants that associate with specific subcellular organelles under different stimulus conditions. These studies should result in identification of the regions of iPLA$_2$β sequence that mediate interaction with an organelle and potentially, to the design of targeted compounds that could enhance or suppress interaction of iPLA$_2$β with a specific organelle.

## Acknowledgments

This research was supported by grants from National Institutes of Health (DK69455, DK34388, P41-RR00954, P60-DK20579, P30-DK56341) and by an Award (to SR) from the American Diabetes Association.

## References

1. Dennis EA. The growing phospholipase A$_2$ superfamily of signal transduction enzymes. Trends Biochem. Sci 1997;22:1–2. [PubMed: 9020581]
2. Gijon MA, Leslie CC. Phospholipases A$_2$. Semin. Cell Dev. Biol 1997;8:297–303. [PubMed: 10024493]
3. Gijon MA, Spencer DM, Kaiser AL, Leslie CC. Role of phosphorylation sites and the C2 domain in regulation of cytosolic phospholipase A$_2$. J. Cell Biol 1999;145:1219–1232. [PubMed: 10366595]
4. Ma Z, Ramanadham S, Wohltmann M, Bohrer A, Hsu FF, Turk J. Studies of insulin secretory responses and of arachidonic acid incorporation into phospholipids of stably transfected insulinoma cells that overexpress group VIA phospholipase A$_2$ (iPLA$_2$β) indicate a signaling rather than a housekeeping role for iPLA$_2$β. J. Biol. Chem 2001;276:13198–13208. [PubMed: 11278673]
5. Mancuso DJ, Jenkins CM, Gross RW. The genomic organization, complete mRNA sequence, cloning, and expression of a novel human intracellular membrane-associated calcium-independent phospholipase A$_2$. J. Biol. Chem 2000;275:9937–9945. [PubMed: 10744668]
6. Ma Z, Turk J. The molecular biology of the group VIA $Ca^{2+}$-independent phospholipase A$_2$. Prog Nucleic Acid Res Mol. Biol 2001;67:1–33. [PubMed: 11525380]
7. Wang Z, Ramanadham S, Ma ZA, Bao S, Mancuso DJ, Gross RW, Turk J. Group VIA Phospholipase A$_2$ forms a signaling complex with the calcium/calmodulin-dependent protein kinase IIβ expressed in pancreatic islet β-cells. J. Biol. Chem 2005;280:6840–6849. [PubMed: 15576376]
8. Seashols SJ, del Castillo Olivares A, Gil G, Barbour SE. Regulation of group VIA phospholipase A$_2$ expression by sterol availability. Biochim. Biophys. Acta (BBA) – Mol. Cell Biol. Lipids 2004;1684:29–37.
9. Ma Z, Wang X, Nowatzke W, Ramanadham S, Turk J. Human pancreatic islets express mRNA species encoding two distinct catalytically active isoforms of group VI phospholipase A$_2$ (iPLA$_2$) that arise from an exon-skipping mechanism of alternative splicing of the transcript from the iPLA$_2$ gene on chromosome 22q13.1. J. Biol. Chem 1999;274:9607–9616. [PubMed: 10092647]
10. Balsinde J, Bianco ID, Ackermann EJ, Conde-Frieboes K, Dennis EA. Inhibition of calciumin-dependent phospholipase A$_2$ prevents arachidonic acid incorporation and phospholipid remodeling in P388D1 macrophages. Proc. Natl. Acad. Sci 1995;92:8527–8531. [PubMed: 7667324]
11. Boilard E, Surette ME. Anti-CD3 and concanavalin A-induced human t cell proliferation is associated with an increased rate of arachidonate-phospholipid remodeling. Lack of involvement of group iv and group VI phospholipase A$_2$ in remodeling and increased susceptibility of proliferating T cells to CoA-independent transacylase inhibitor-induced apoptosis. J. Biol. Chem 2001;276:17568–17575. [PubMed: 11278296]
12. Isenovic E, LaPointe MC. Role of $Ca^{2+}$-Independent phospholipase A$_2$ in the regulation of inducible nitric oxide synthase in cardiac myocytes. Hypertension 2000;35:249–254. [PubMed: 10642306]
13. Maggi LB Jr, Moran JM, Scarim AL, Ford DA, Yoon J-W, McHowat J, Buller RML, Corbett JA. Novel role for calcium-independent phospholipase A$_2$ in the macrophage antiviral response of inducible nitric-oxide synthase expression. J. Biol. Chem 2002;277:38449–38455. [PubMed: 12167650]

14. Moran JM, Buller RML, McHowat J, Turk J, Wohltmann M, Gross RW, Corbett JA. Genetic and pharmacologic evidence that calcium-independent phospholipase $A_2\beta$ regulates virus-induced inducible nitric-oxide synthase expression by macrophages. J. Biol. Chem 2005;280:28162–28168. [PubMed: 15946940]
15. Tithof PK, Olivero J, Ruehle K, Ganey PE. Activation of neutrophil calcium-dependent and -independent phospholipases $A_2$ by organochlorine compounds. Toxicol. Sci 2000;53:40–47. [PubMed: 10653519]
16. Williams SD, Ford DA. Calcium-independent phospholipase $A_2$ mediates CREB phosphorylation and *c-fos* expression during ischemia. Am. J. Physiol. Heart Circ. Physiol 2001;281:H168–H176. [PubMed: 11406482]
17. Bao S, Miller DJ, Ma Z, Wohltmann M, Eng G, Ramanadham S, Moley K, Turk J. Male mice that do not express group VIA phospholipase $A_2$ produce spermatozoa with impaired motility and have greatly reduced fertility. J. Biol. Chem 2004;279:38194–38200. [PubMed: 15252026]
18. Ramanadham S, Yarasheski KE, Silva MJ, Wohltmann M, Novack DV, Christiansen B, Tu X, Zhang S, Lei X, Turk J. Age-related changes in bone morphology are accelerated in group VIA phospholipase $A_2$ ($iPLA_2\beta$)-null mice. Am. J. Pathol 2008;172:868–881. [PubMed: 18349124]
19. Carper MJ, Zhang S, Turk J, Ramanadham S. Skeletal muscle group VIA phospholipase $A_2$ ($iPLA_2\beta$): Expression and role in fatty acid oxidation. Biochemistry 2008;47:12241. [PubMed: 18937505]
20. St-Gelais F, Menard C, Congar P, Trudeau LE, Massicotte G. Postsynaptic injection of calcium-independent phospholipase $A_2$ inhibitors selectively increases AMPA receptor-mediated synaptic transmission. Hippocampus 2004;14:319–325. [PubMed: 15132431]
21. Schaeffer EL, Gattaz WF. Inhibition of calcium-independent phospholipase $A_2$ activity in rat hippocampus impairs acquisition of short- and long-term memory. Psychopharmacology (Berl) 2005;181:392–400. [PubMed: 15830227]
22. Mendes CT, Gattaz WF, Schaeffer EL, Forlenza OV. Modulation of phospholipase $A_2$ activity in primary cultures of rat cortical neurons. J. Neural. Transm 2005;112:1297–1308. [PubMed: 15682269]
23. Berti-Mattera LN, Harwalkar S, Hughes B, Wilkins PL, Almhanna K. Proliferative and morphological effects of endothelins in Schwann cells: roles of p38 mitogen-activated protein kinase and $Ca^{2+}$-independent phospholipase $A_2$. J. Neurochem 2001;79:1136–1148. [PubMed: 11752055]
24. Biancheri R, Rossi A, Alpigiani G, Filocamo M, Gandolfo C, Lorini R, Minetti C. Cerebellar atrophy without cerebellar cortex hyperintensity in infantile neuroaxonal dystrophy (INAD) due to PLA2G6 mutation. Eur. J. Paediatr. Neurol 2007;11:175–177. [PubMed: 17254819]
25. Westaway SK, Gregory A, Hayflick SJ. Mutations in PLA2G6 and the riddle of Schindler disease. J. Med. Genet 2007;44:e64. [PubMed: 17209134]
26. Junqueira R, Cordeiro Q, Meira-Lima I, Gattaz WF, Vallada H. Allelic association analysis of phospholipase $A_2$ genes with schizophrenia. Psychiatr. Genet 2004;14:157–160. [PubMed: 15318030]
27. Smesny S, Kinder D, Willhardt I, Rosburg T, Lasch J, Berger G, Sauer H. Increased calcium-independent phospholipase $A_2$ activity in first but not in multiepisode chronic schizophrenia. Biol. Psychiatry 2005;57:399–405. [PubMed: 15705356]
28. Boittin FX, Petermann O, Hirn C, Mittaud P, Dorchies OM, Roulet E, Ruegg UT. $Ca^{2+}$-independent phospholipase $A_2$ enhances store-operated $Ca^{2+}$ entry in dystrophic skeletal muscle fibers. J. Cell Sci 2006;119:3733–3742. [PubMed: 16926189]
29. Gong MC, Arbogast S, Guo Z, Mathenia J, Su W, Reid MB. Calcium-independent phospholipase $A_2$ modulates cytosolic oxidant activity and contractile function in murine skeletal muscle cells. J. Appl. Physiol 2006;100:399–405. [PubMed: 16166238]
30. Kan H, Xie Z, Finkel MS. $iPLA_2$ inhibitor blocks negative inotropic effect of HIV gp120 on cardiac myocytes. J. Mol. Cell. Cardiol 2006;40:131–137. [PubMed: 16316660]
31. Ronkko S, Rekonen P, Kaarniranta K, Puustjarvi T, Terasvirta M, Uusitalo H. Phospholipase $A_2$ in chamber angle of normal eyes and patients with primary open angle glaucoma and exfoliation glaucoma. Mol. Vis 2007;13:408–417. [PubMed: 17417602]

32. Gilroy DW, Newson J, Sawmynaden P, Willoughby DA, Croxtall JD. A novel role for phospholipase $A_2$ isoforms in the checkpoint control of acute inflammation. FASEB J 2004;18:489–498. [PubMed: 15003994]
33. Ramanadham S, Gross RW, Han X, Turk J. Inhibition of arachidonate release by secretagogue-stimulated pancreatic islets suppresses both insulin secretion and the rise in beta-cell cytosolic calcium ion concentration. Biochemistry 1993;32:337–346. [PubMed: 8418854]
34. Ramanadham S, Song H, Hsu FF, Zhang S, Crankshaw M, Grant GA, Newgard CB, Bao S, Ma Z, Turk J. Pancreatic islets and insulinoma cells express a novel isoform of group VIA phospholipase $A_2$ (iPLA$_2$β) that participates in glucose-stimulated insulin secretion and is not produced by alternate splicing of the iPLA$_2$β transcript. Biochemistry 2003;42:13929–13940. [PubMed: 14636061]
35. Ramanadham S, Wolf MJ, Jett PA, Gross RW, Turk J. Characterization of an ATP-stimulatable $Ca^{2+}$-independent phospholipase $A_2$ from clonal insulin-secreting HIT cells and rat pancreatic islets: a possible molecular component of the beta-cell fuel sensor. Biochemistry 1994;33:7442–7452. [PubMed: 8003509]
36. Ramanadham S, Wolf MJ, Li B, Bohrer A, Turk J. Glucose-responsitivity and expression of an ATP-stimulatable, $Ca^{2+}$-independent phospholipase $A_2$ enzyme in clonal insulinoma cell lines. Biochim. Biophys. Acta 1997;1344:153–164. [PubMed: 9030192]
37. Ramanadham S, Hsu FF, Zhang S, Jin C, Bohrer A, Song H, Bao S, Ma Z, Turk J. Apoptosis of insulin-secreting cells induced by endoplasmic reticulum stress is amplified by overexpression of group VIA calcium-independent phospholipase $A_2$ (iPLA$_2$β) and suppressed by inhibition of iPLA$_2$β. Biochemistry 2004;43:918–930. [PubMed: 14744135]
38. Lei X, Zhang S, Bohrer A, Bao S, Song H, Ramanadham S. The Group VIA calcium-independent phospholipase $A_2$ participates in ER stress-induced INS-1 insulinoma cell apoptosis by promoting ceramide generation via hydrolysis of sphingomyelins by neutral sphingomyelinase. Biochemistry 2007;46:10170–10185. [PubMed: 17685585]
39. Lei X, Zhang S, Bohrer A, Ramanadham S. Calcium-independent phospholipase $A_2$ (iPLA$_2$β)-mediated ceramide generation plays a key role in the cross-talk between the endoplasmic reticulum (ER) and mitochondria during er stress-induced insulin-secreting cell apoptosis. J. Biol. Chem 2008;283:34819–34832. [PubMed: 18936091]
40. Bao S, Song H, Wohltmann M, Ramanadham S, Jin W, Bohrer A, Turk J. Insulin secretory responses and phospholipid composition of pancreatic islets from mice that do not express group VIA phospholipase $A_2$ and effects of metabolic stress on glucose homeostasis. J. Biol. Chem 2006;281:20958–20973. [PubMed: 16732058]
41. Bao S, Bohrer A, Ramanadham S, Jin W, Zhang S, Turk J. Effects of stable suppression of group VIA phospholipase $A_2$ expression on phospholipid content and composition, insulin secretion, and proliferation of INS-1 insulinoma cells. J. Biol. Chem 2006;281:187–198. [PubMed: 16286468]
42. Bao S, Jacobson DA, Wohltmann M, Bohrer A, Jin W, Philipson LH, Turk J. Glucose homeostasis, insulin secretion, and islet phospholipids in mice that overexpress iPLA$_2$β in pancreatic β-cells and in iPLA$_2$β-null mice. Am. J. Physiol. Endocrinol. Metab 2008;294:E217–E229. [PubMed: 17895289]
43. Ma Z, Bohrer A, Wohltmann M, Ramanadham S, Hsu F-F, Turk J. Studies of phospholipid metabolism, proliferation, and secretion of stably transfected insulinoma cells that overexpress group VIA phospholipase $A_2$. Lipids 2001;36:689–700. [PubMed: 11521967]
44. Ramanadham S, Hsu F-F, Bohrer A, Ma Z, Turk J. Studies of the role of group vi phospholipase $A_2$ in fatty acid incorporation, phospholipid remodeling, lysophosphatidylcholine generation, and secretagogue-induced arachidonic acid release in pancreatic islets and insulinoma cells. J. Biol. Chem 1999;274:13915–13927. [PubMed: 10318801]
45. Ma Z, Zhang S, Turk J, Ramanadham S. Stimulation of insulin secretion and associated nuclear accumulation of iPLA$_2$β in INS-1 insulinoma cells. Am. J. Physiol. Endocrinol. Metab 2002;282:E820–E833. [PubMed: 11882502]
46. Bao S, Jin C, Zhang S, Turk J, Ma Z, Ramanadham S. Beta-cell calcium-independent group VIA phospholipase $A_2$ (iPLA$_2$β): Tracking iPLA$_2$β movements in response to stimulation with insulin secretagogues in INS-1 cells. Diabetes 2004;53:S186–S189. [PubMed: 14749286]
47. Cormack BP, Valdivia RH, Falkow S. FACS-optimized mutants of the green fluorescent protein (GFP). Gene 1996;173:33–38. [PubMed: 8707053]

48. Gross RW, Ramanadham S, Kruszka KK, Han X, Turk J. Rat and human pancreatic islet cells contain a calcium ion independent phospholipase $A_2$ activity selective for hydrolysis of arachidonate which is stimulated by adenosine triphosphate and is specifically localized to islet beta-cells. Biochemistry 1993;32:327–336. [PubMed: 8418853]
49. Bao S, Li Y, Lei X, Wohltmann M, Jin W, Bohrer A, Semenkovich CF, Ramanadham S, Tabas I, Turk J. Attenuated free cholesterol loading-induced apoptosis but preserved phospholipid composition of peritoneal macrophages from mice that do not express group VIA phospholipase $A_2$. J. Biol. Chem 2007;282:27100–27114. [PubMed: 17627946]
50. Song H, Hecimovic S, Goate A, Hsu FF, Bao S, Vidavsky I, Ramanadham S, Turk J. Characterization of N-terminal processing of group VIA phospholipase $A_2$ and of potential cleavage sites of amyloid precursor protein constructs by automated identification of signature peptides in LC/MS/MS analyses of proteolytic digests. J. Am. Soc. Mass Spectrom 2004;15:1780–1793. [PubMed: 15589755]
51. Ramanadham S, Hsu F, Zhang S, Bohrer A, Ma Z, Turk J. Electrospray ionization mass spectrometric analyses of phospholipids from INS-1 insulinoma cells: comparison to pancreatic islets and effects of fatty acid supplementation on phospholipid composition and insulin secretion. Biochim. Biophys. Acta 2000;1484:251–266. [PubMed: 10760474]
52. Ma Z, Ramanadham S, Kempe K, Chi XS, Ladenson J, Turk J. Pancreatic islets express a $Ca^{2+}$-independent phospholipase $A_2$ enzyme that contains a repeated structural motif homologous to the integral membrane protein binding domain of ankyrin. J. Biol. Chem 1997;272:11118–11127. [PubMed: 9111008]
53. Ma Z, Ramanadham S, Hu Z, Turk J. Cloning and expression of a group IV cytosolic $Ca^{2+}$-dependent phospholipase $A_2$ from rat pancreatic islets. Comparison of the expressed activity with that of an islet group VI cytosolic $Ca^{2+}$-independent phospholipase $A_2$. Biochim. Biophys. Acta 1998;1391:384–400. [PubMed: 9555100]
54. Fatima S, Yaghini FA, Ahmed A, Khandekar Z, Malik KU. CaM kinase IIα mediates norepinephrine-induced translocation of cytosolic phospholipase $A_2$ to the nuclear envelope. J. Cell Sci 2003;116:353–365. [PubMed: 12482921]
55. Kim YJ, Kim KP, Rhee HJ, Das S, Rafter JD, Oh YS, Cho W. Internalized group V secretory phospholipase $A_2$ acts on the perinuclear membranes. J. Biol. Chem 2002;277:9358–9365. [PubMed: 11777916]
56. Evans JH, Spencer DM, Zweifach A, Leslie CC. Intracellular calcium signals regulating cytosolic phospholipase $A_2$ translocation to internal membranes. J. Biol. Chem 2001;276:30150–30160. [PubMed: 11375391]
57. Ramanadham S, Song H, Bao S, Hsu F-F, Zhang S, Ma Z, Jin C, Turk J. Islet complex lipids: Involvement in the actions of group VIA calcium-independent phospholipase $A_2$ in β-Cells. Diabetes 2004;53:S179–S185. [PubMed: 14749285]

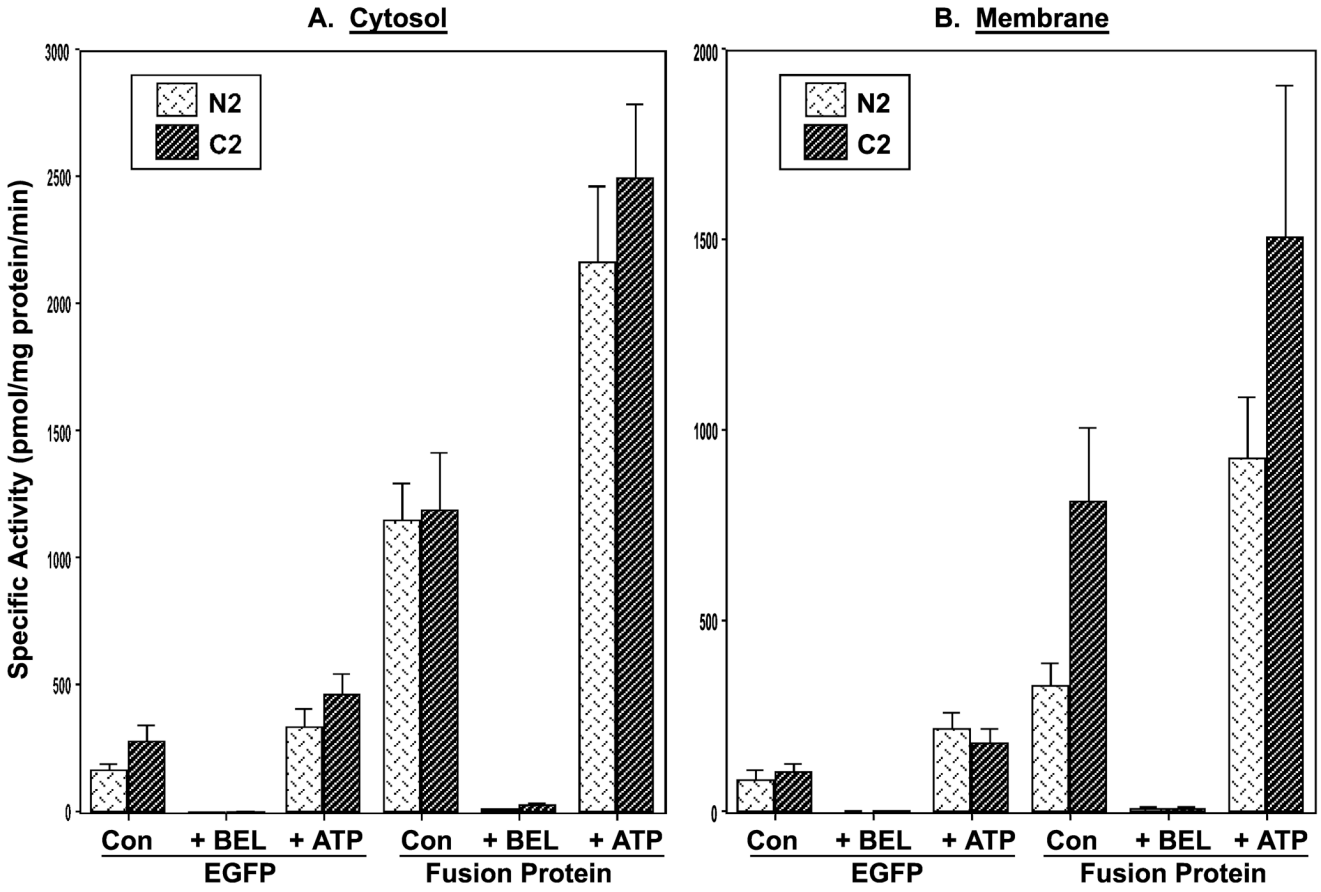


**Fig. 1. iPLA$_2$β enzymatic activity in stably-transfected INS-1 cells**

Specific iPLA$_2$β enzymatic activity in 25 μg protein aliquots of cytosol or membranes, prepared from transfected INS-1 cells, was assayed and quantitated as described in Methods. The data are presented as mean ± SEM (n = 8–10). A: Cytosolic activity. B: Membrane-associated activity.

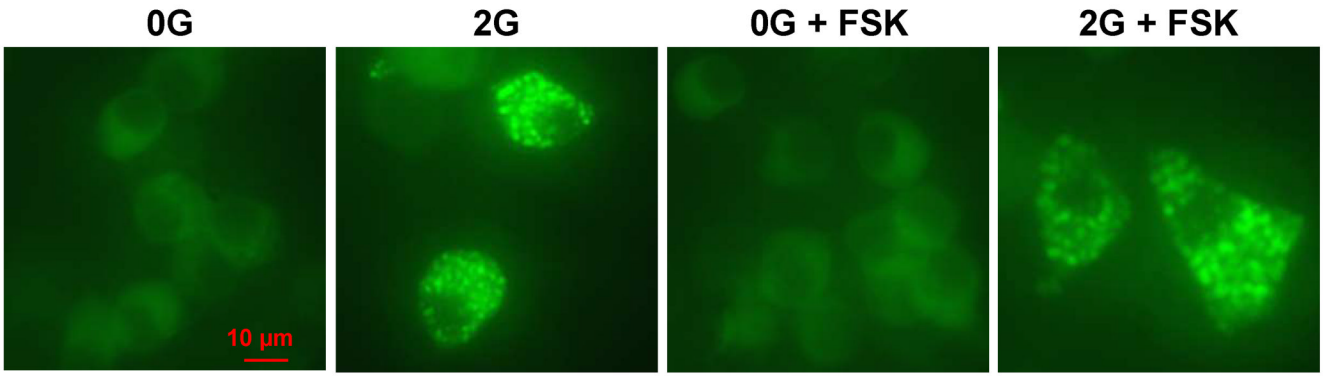


**Fig. 2. Secretagogue-stimulated localization of fusion protein in INS-1 cells**

INS-1 cells expressing fpC2 (EGFP-iPLA$_2$β) were incubated with glucose (G, 0 or 2 mM) in the absence and presence of forskolin (FSK, 2.5 μM). At 2 h, iPLA$_2$β protein localization was monitored by fluorescence microscopy.

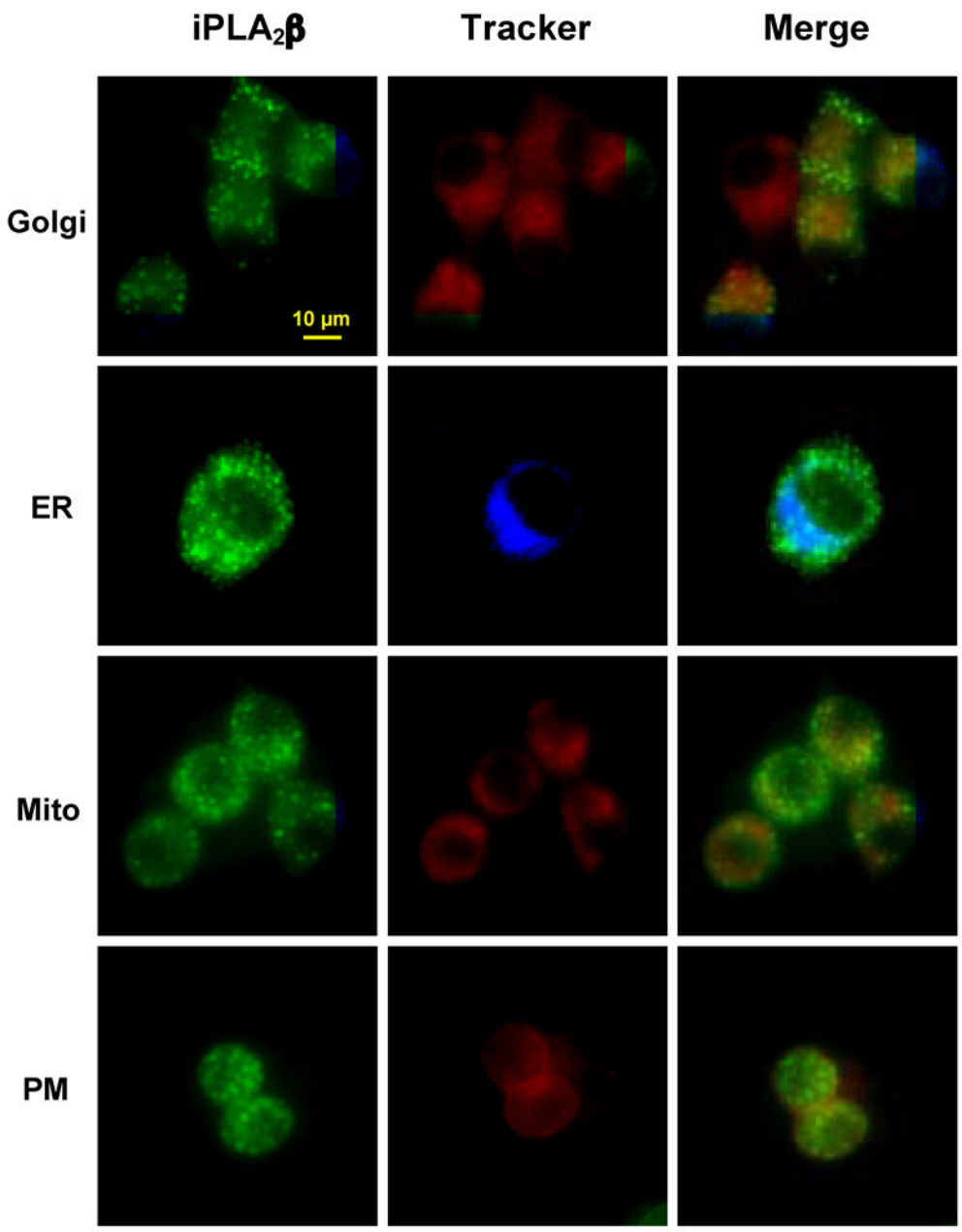


**Fig. 3. Secretagogue-stimulated subcellular distribution of fusion protein**

INS-1 cells expressing fpC2 (EGFP-iPLA$_2$β) were incubated with glucose (G, 2 mM) and forskolin (FSK, 2.5 μM) along with organelle markers for Golgi (5 μM) or ER (600 nM), as described in Methods. At 2 h following stimulation, the EGFP (FITC) fluorescence was monitored separately from fluorescence associated with organelle Tracker; Golgi (rhodamine), ER (DAPI), mitochondria (rhodamine) and plasma membrane (PM, rhodamine). *Left Panels*, EGFP-associated iPLA$_2$β fluorescence alone; *Middle Panels*, organelle Tracker fluorescence alone; and *Right Panels*, overlay of EGFP and organelle Tracker fluorescences.

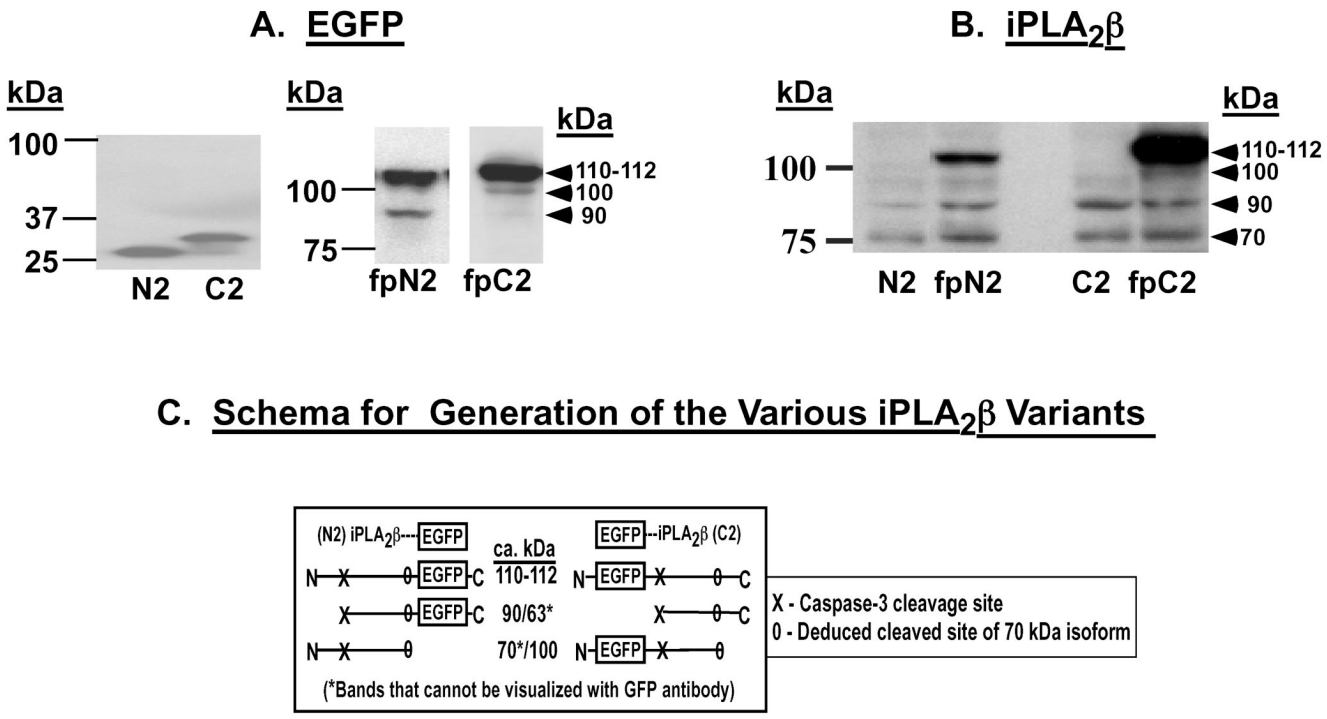


**Fig. 4. EGFP and iPLA$_2$β immunoblotting analyses in INS-1 cells**

Following transfection of INS-1 cells with constructs encoding EGFP ± iPLA$_2$β, cytosol protein fractions were prepared and analysed by SDS-PAGE and transferred onto Immobolin-P PVDF membrane. The electroblots were probed with antibodies directed against EGFP or iPLA$_2$β and immunoreactive protein bands were visualized by ECL. A: EGFP immunoblotting. B: iPLA$_2$β immunoblotting. C: Proposed scheme for generation and visualization of iPLA$_2$β variants. (N2, EGFP-N2 vector only; C2, EGFP-C2 vector only; fpN2, iPLA$_2$β-EGFP; fpC2, and EGFP- iPLA$_2$β.)

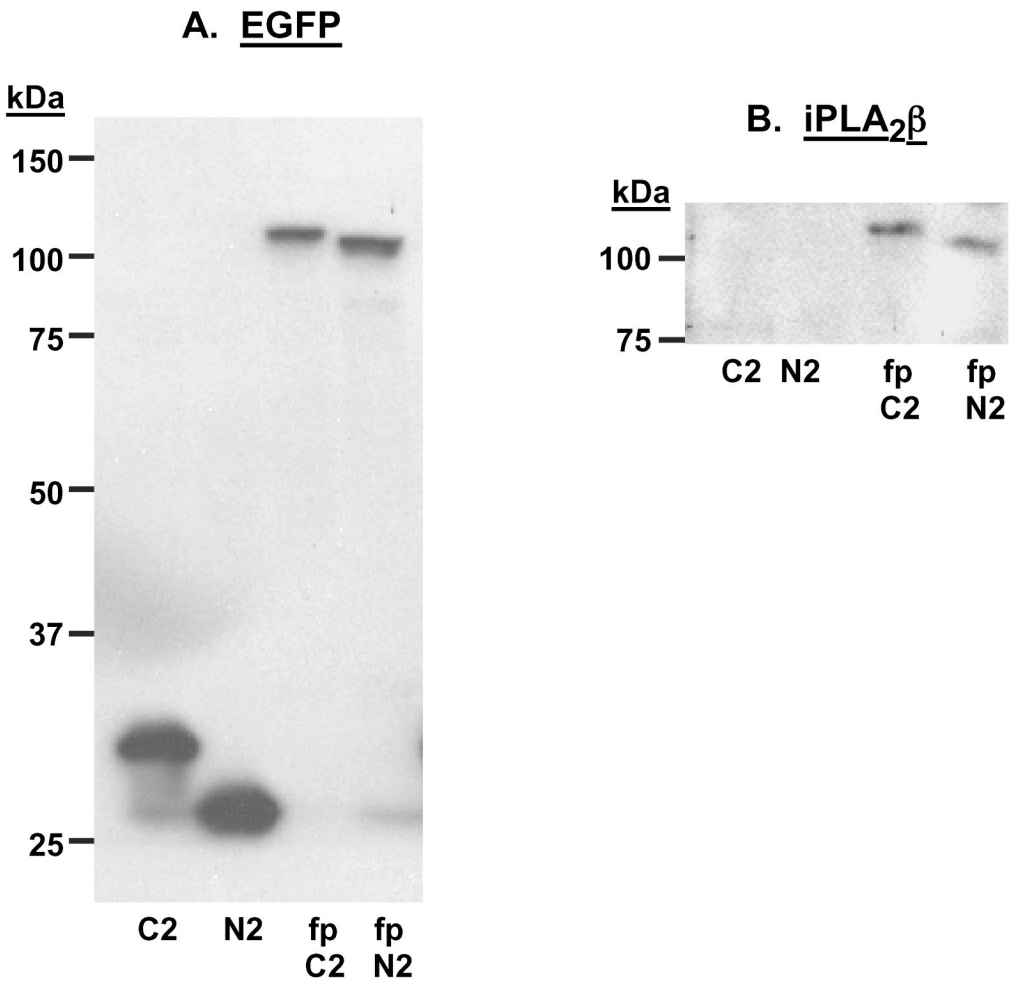


**Fig. 5. Immunoblotting analyses of plasma membrane-associated iPLA$_2$β**

Plasma membrane protein fractions were prepared and analysed by SDS-PAGE and transferred onto Immobolin-P PVDF membrane. The electroblots were probed with antibodies directed against EGFP or iPLA$_2$β and the immunoreactive protein bands were visualized by ECL. A: EGFP immunoblotting. B: iPLA$_2$β immunoblotting.

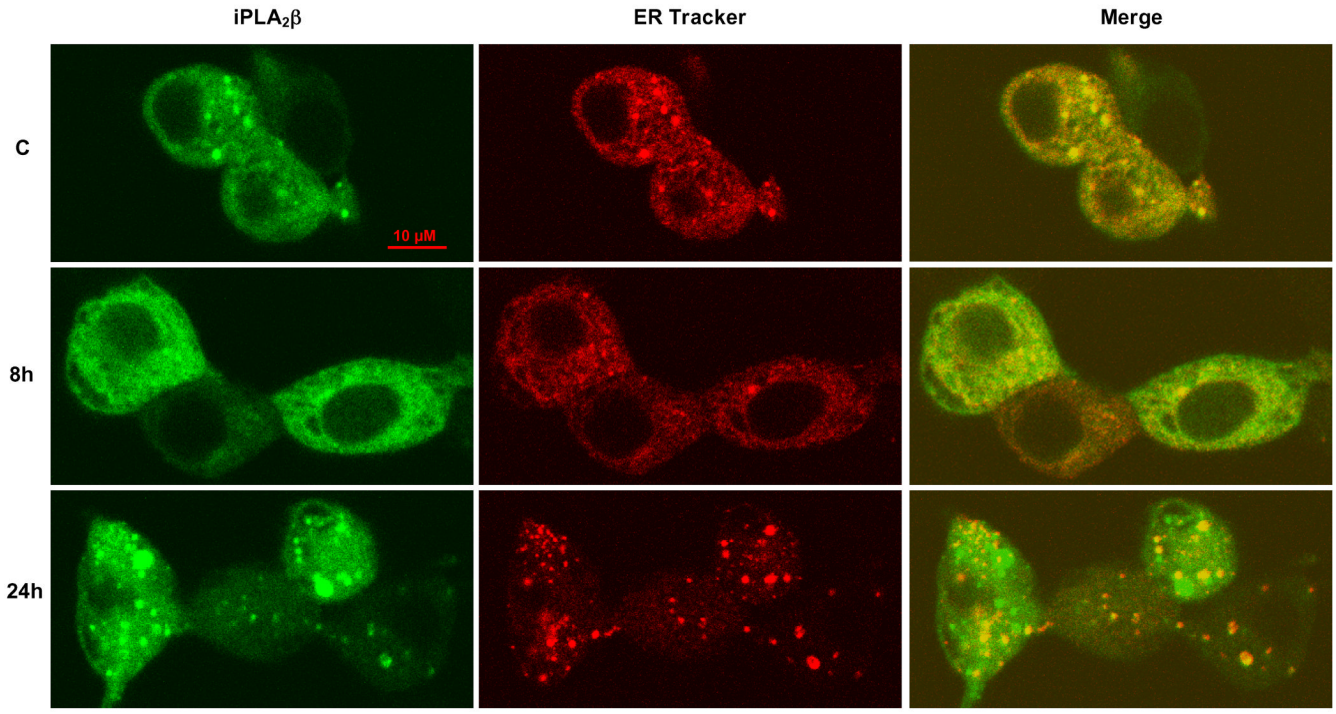


**Fig. 6. iPLA$_2$β association with the ER following induction of ER stress in INS-1 cells**

INS-1 cells expressing fpC2 (EGFP-iPLA$_2$β) alone or fpC2 along with a fusion protein of ER-targeting sequence of calreticulin tagged to the N-terminus of MonoRed were treated with DMSO vehicle (Con) or with thapsigargin (0.5 μM) to induce ER stress. At 8 and 24 h the cells were harvested, fixed, and assessed by fluorescence microscopy. Images of individual fluorescence associated with iPLA$_2$β (left panels) and ER marker (middle panels) and the merged fluorescence (right panels) are presented.

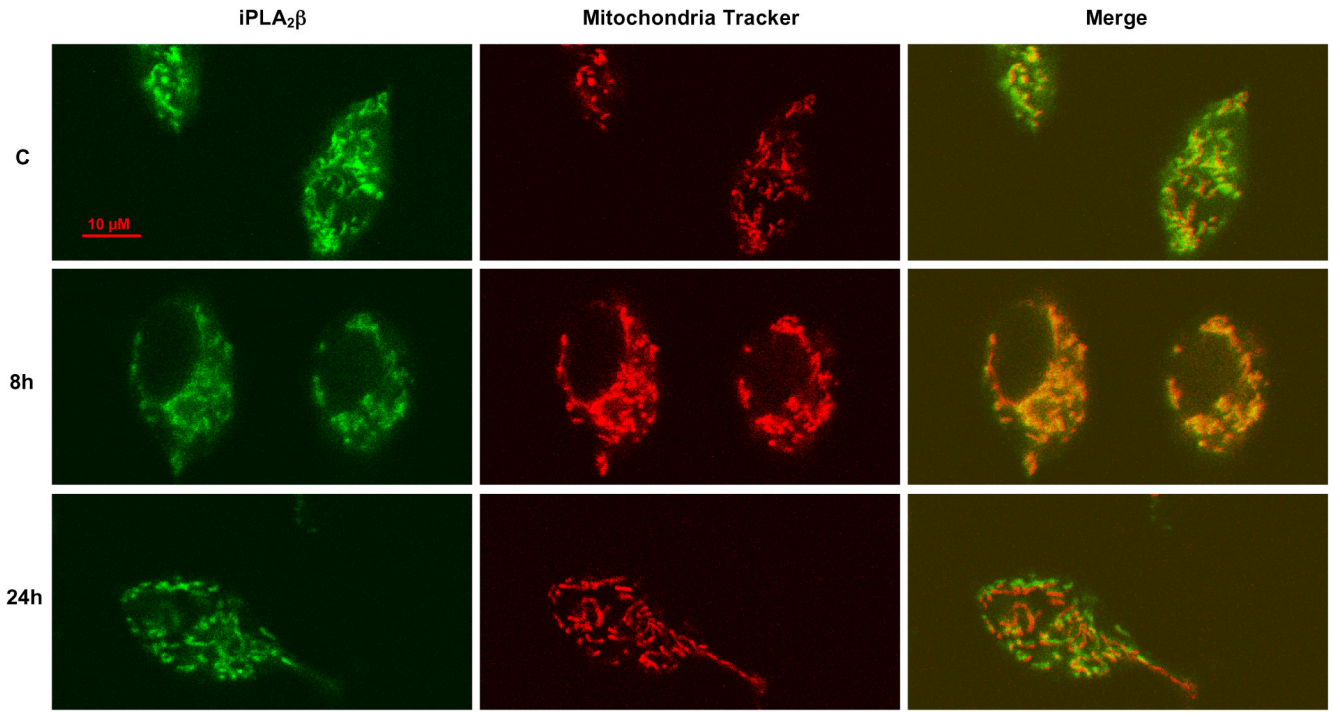


**Fig. 7. ER stress-induced accumulation of iPLA$_2$β in INS-1 cell mitochondria**

INS-1 cells expressing fpC2 (EGFP-iPLA$_2$β) alone or fpC2 along with a fusion protein of mitochondrial-targeting sequence of human cytochrome *c* oxidase subunit VIII tagged to *Discosoma sp.* red fluorescent protein were treated with DMSO vehicle (Con) or with thapsigargin (0.5 μM) to induce ER stress. At 8 and 24 h the cells were harvested, fixed, and assessed by fluorescence microscopy. Images of individual fluorescence associated with iiPLA$_2$β (left panels) and mitochondria marker (middle panels) and the merged fluorescence (right panels) are presented.

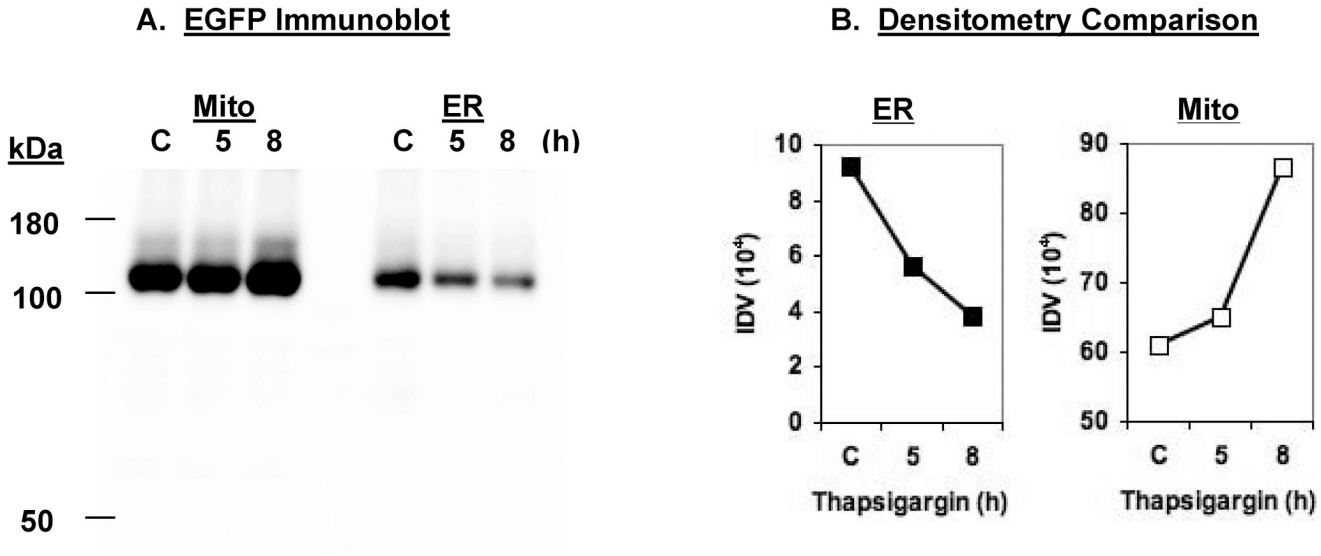


**Fig. 8. ER stress-induced accumulation of iPLA$_2$β isoforms in the ER and mitochondria**

INS-1 cells overexpressing fpN2 (iPLA$_2$β-EGFP) were treated with vehicle (DMSO) alone or thapsigargin (1 μM, 37 °C) for 5 or 8 h. The cells were harvested and mitochondria and ER fractions prepared and aliquots (30 μg protein) of the fractions were analysed by SDS-PAGE (7.5 %) and processed for EGFP immunblotting analyses. A: EGFP Immnoublot B: Denistometry comparison. (Mito, mitochondria; and ER, endoplasmic reticulum; IDV, Integrated Density Value).

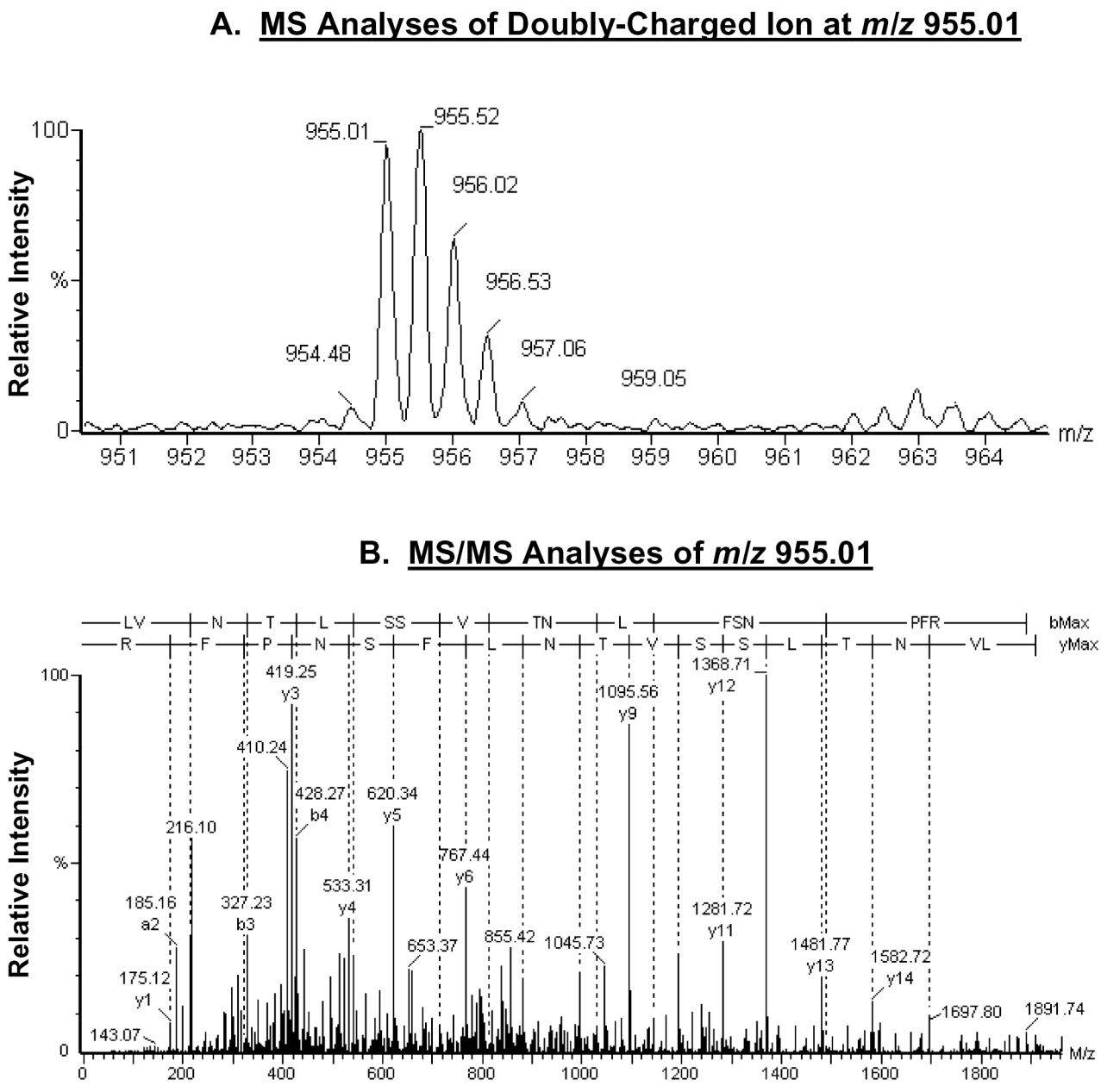


**Fig. 9. Analyses of fragment ion with *m/z* of 955.01 arising from tryptic digestion of iPLA$_2$β by mass spectrometry**

ATP affinity chromatography was used to purify iPLA$_2$β from INS-1 cells overexpressing iPLA$_2$β. Fractions containing iPLA$_2$β catalytic activity were pooled, concentrated, and the concentrate was resolved by SDS-PAGE. Protein band migrating with an apparent molecular mass of 84 kDa corresponding to iPLA$_2$β was identified by Coomassie staining, excised, and processed for digestion with trypsin. The tryptic digest was then analyzed by mass spectrometry. A: MS spectrum of doubly charged ion with *m/z* 955.01. B: Tandem MS spectrum of precursor ion with *m/z* 955.01.

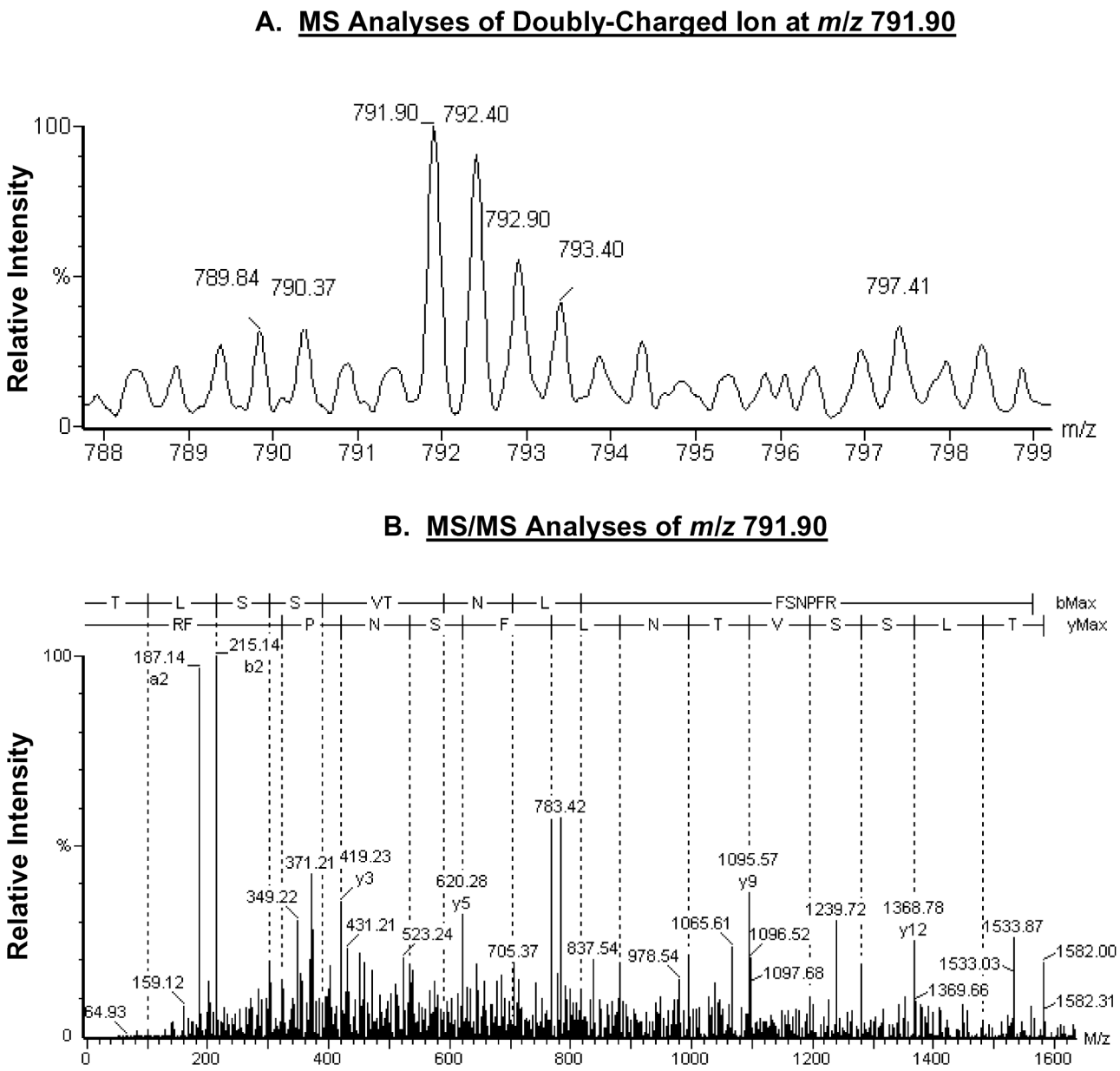


**Fig. 10. Analyses of fragment ion with *m/z* of 791.90 arising from tryptic digestion of iPLA$_2$β by mass spectrometry**

Tryptic digest of iPLA$_2$β was prepared as described for Fig. 9 and analysed by mass spectrometry. A: MS spectrum of doubly charged ion with *m/z* 791.90. B: Tandem MS spectrum of precursor ion with *m/z* 791.90.